Extended Abstracts of the 2011 International Conference on Solid State Devices and Materials, Nagoya, 2011, pp142-143

Characterization and improved endurance for HfO_2 resistive memory with CMP treated TiN bottom electrode

Pang-Shiu Chen, Yu-Sheng Chen[1,2], Heng-Yuan Lee[1], Tai-Yuan Wu[1], Wen-Hsing Liu[1], Pei-Yi Gu[1], Fred Chen[1], and Ming-Jinn Tsai[1]

Department of Chemical and Materials Engineering, MingShin University of Science & Technology Hsinfong, Hsinchu 304, Taiwan, [1]Industrial Technology Research Institute, Hsinchu 310, Taiwan, [2]Institute of Electronics Engineering, National Tsing Hua University, Hsinchu 300, Taiwan, Phone : 886-3-5593142 ext 3377, Fax : 886-3-5593142, E-mail :pschen@must.edu.tw

1. Introduction

Recently, binary oxide resistive memories (RM) with simple device structure, excellent scalability, and low power consumption, are considered as one of attractive candidates for next generation nonvolatile memory [1]. The authors proposed a reactive Ti overlayer to modify the dielectric strength of HfO_2 film [2]. The Ti/HfO_2 RMs exhibit excellent bipolar resistive switching (BRS) with good retention and high speed as fast as 0.3 ns. Meanwhile, the surface roughness and stoichiometries of electrode were reported to influence the electrical properties of metal-insulator-metal capacitor [3,4]. We also adopted chemical mechanical polish (CMP) to flatten the bottom electrode (BE) [5], the endurance of the Ti/HfO_2 RM devices with a series transistor (1T1R) was greatly improved. However, the effects of CMP treated TiN BE on the structure of HfOx overlayer and the electrical properties one RM or 1T1R are still unclear. In this work, we comprehensive studied the impacts of CMP treated BE (CBE) on the microstructure and memory performance of HfO_2 based RM. A series resistor or a transistor was used to the endurance reliability of Ti/HfO_2 based RM with CBE by suppressing the current overshoot during forming/set step.

2. Device Fabrication and measurement

The bipolar RM devices were prepared through the stacked layers, which consisted of Ti/HfO_2. TiN layer by sputtering were served as top electrode (TE) and BE, the detail process can be checked elsewhere [2], atomic layer deposition were adopted to deposit HfOx films of 5 nm-thick. The BE in some samples are treated with CMP process to smoothen the TiN layer, then regrow TiN to be the default thickness (50 nm). Some of the stacked films were annealed at post-metal annealing (PMA) of 450 °C for 5 min. The microstructure of the stacked structure was investigated by cross-sectional transmission electron microscopy (XTEM) operated at 200 *keV*. Grazing incident-angle X-ray diffraction (GIAXRD) was adopted to characterize the crystal structure of HfOx films before/after PMA. X-ray photoelectron spectroscopy (XPS) was used to analyze the composition depth profile of the stacked layer. The memory devices with or without CBE with cell size ranging from 0.13 to 60 μm^2 were fabricated, the devices are referred as 1R ones. A series resistor or transistor based on 0.18 μm technology was used to suppress the overshooting current in some devices (1T1R) during the forming process. The current-voltage (*I-V*) were characterized by using HP 4156A in sweep mode. 50 devices were measured to examine their electrical uniformity. The endurance of the 1R and 1T1R was studied by the stress mode of HP 4156A and pulse mode of 81110A.

3. Results and Discussion

The HRTEM micrograph of Ti/HfOx stacked layer upon BE and CBE under PMA are presented in Fig. 1. In the Fig. 1(b), there are some blurred regions at the interface of HfOx and CBE. The thickness of HfOx in both cases are the same, this results suggests that the growth rate of HfOx by ALD seems insensitive on the roughness of TiN BE. In Fig. 2, the crystallinity of HfOx films on different TiN BE before/after PMA were explored by GIAXRD. For the as-prepared sample with CBE, the crystal structure of HfOx is amorphous. After PMA, the X-ray spectrum for the sample with CBE is partially crystalline, which is similar to that without CMP. But, the intensity of X-ray spectra originated from HfOx film upon CBE is lower than the latter. The surface roughness of the sample with TiN BE is ~ 1.1 nm, which is higher than that of CBE one (0.3 nm) as shown in Fig. 3. Oxygen (O) atoms distribution in as-grown and PMA for the sample of Ti/HfOx above CBE are depicted in Fig. 4. The Ti layer can effectively getter a lots of O atoms with the assistance of the successive PMA. In Fig. 5, the typical curves of leakage current and applied voltage for the 5-μm pristine RM with CBE from 27 to 180 °C are depicted. The inserted one shows the dependence of current density @ 1 *V* on the measurement temperature. A double logarithmic *I-V* curve for the devices is presented in the insert figure of Fig. 6. At low bias (< 0.15 *V*), the carriers obey ohmic behavior and are dominated by space charge limited conduction (SCLC) under the bias between 0.15 and 0.35 *V*. At high E-field, the carriers follow the Fowler-Nordheim (F-N) tunneling. The CMP devices show a better time dependent to breakdown property than that without CBE. The typical forming process and first reset *I-V* curves for the devices are shown (Fig. 7), the inserted one exhibits the typical BRS of the devices. The Weibull plots of the forming voltage (V_F) distribution for the devices are presented in Fig. 8. In Fig. 9, the Weibull plot of the resistance of initial resistance state (IRS) and first RESET for the devices are presented. Owing to a high IRS magnitude of HfOx insulator with CBE, the RMs have a relative high V_F (~ 2 V) and the lower resistance of first low resistance state (LRS) than that without CBE (Fig. 7). But the SET voltage and RESET voltage of the RM devices seem to be insensitive to the BE roughness (not shown here). The resistance of HRS and LRS for the device without CBE can be well resolved with a high resistance ratio (> 100) after 3×10^5 cycles as shown in Fig. 10. In contrast, the endurance of HfOx RM by using CBE is presented in Fig. 11. The HRS was degraded and both of the memory states for the device will merge after 10^3 cycles. The excessive overshooting current in the RM during the forming or set step is responsible for this result. The excessive overshooting current in the CMP device with a series resistor (~ 800 Ω) can be suppressed during the forming (not shown here), but the memory window of endurance for the devices are improved (> 10^4 cycles, not shown here). With a series transistor as a perfect current limiter, the overshooting current in the CMP device during the repetitive forming/SET step can be effectively eliminated. Endurance of HfOx RMs with 1T1R configuration by using CBE in Fig. 12, the repetitive on/off states with 40 ns switching speed can exceed up to 5×10^7 cycles.

4. Conclusions

The microstructure of HfOx upon TiN with CMP and without CMP BE were investigated. Some nanocrystals embedded in amorphous matrix were observed in the HfOx films on CBE under PMA. CMP treated BE leads to the RM devices with high V_F, low IRS current and low first LRS magnitude. High V_F and the current overshoot may damage the HfOx RMs to suffer unstable switching during cycling test. The RM with an 800 Ω series resistor can enhance their endurance by alleviate the excessive overshooting current during forming. A series transistor as the selection device can suppress the current during the successive forming/SET step, the RMs with CBE show robust programming/erasing during the endurance test (> 5×10^7 cycles).

5. References

[1] Z. Wei *et al.*, *IEDM Tech. Dig.*, p. 293, 2008. [2] Y. S. Chen *et al. IEDM Tech. Dig.*, p. 297, 2009. [3] G. Jegert, J. Appl. Phys. 109, 014504, 2011. [4] Y. Otani *et al.* VLSI-tsa p. 104, 2011. [5] H. Y. Lee *et al. IEDM Tech. Dig.*, p. 297, 2009.

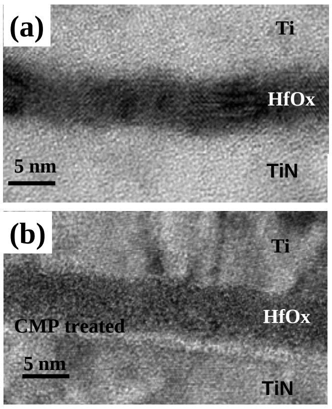

Fig. 1. HRTEM images of Ti/HfOx above (a) TiN and (b) CMP treated TiN stacked layer under PMA of 450 °C for 5 min.

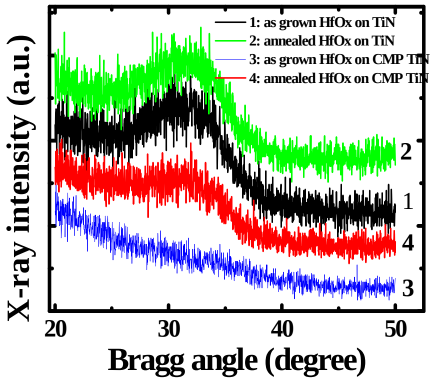

Fig. 2. The GIAXRD spectra for as-prepared and PMA Ti/HfOx above TiN and CMP treated TiN BE.

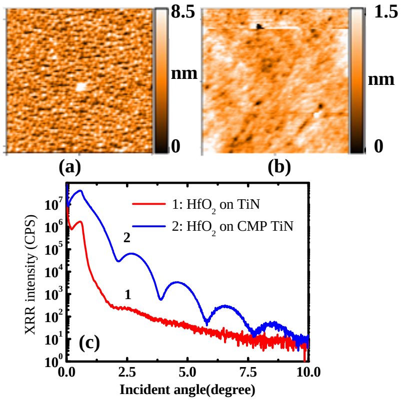

Fig. 3. (a) AFM images of annealed HfOx above (a) TiN and (b) CMP TiN BE, (c) the XRR spectra of CBE samples.

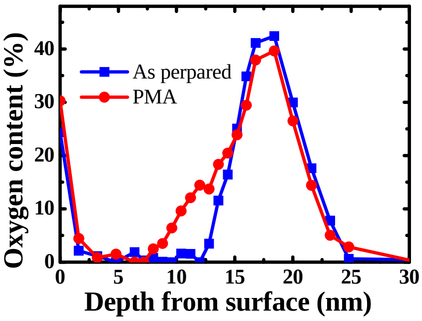

Fig. 4. Oxygen atoms distribution in as-grown and PMA for the sample of TiN/Ti/HfOx above CMP treated TiN BE.

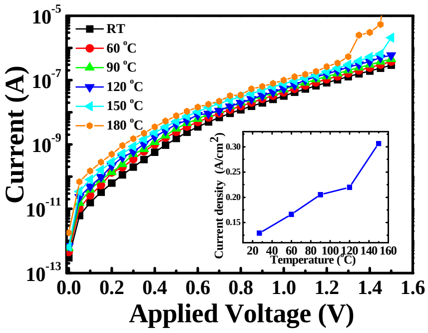

Fig. 5. The typical leakage current and applied voltage curves for the device with CBE from 27 to 180 °C. The inserted one shows the dependence of current density @ 1 V on the measurement temperature.

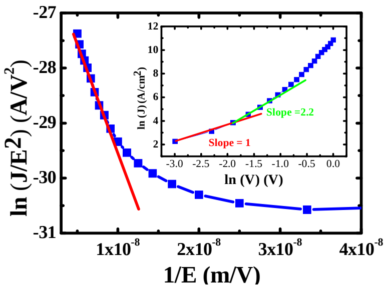

Fig. 6. F-N tunneling plot of initial states at RT for the pristine device with CMP BE. The inserted one shows the double logarithmic *I-V* plot for the same devices at low electrical field region.

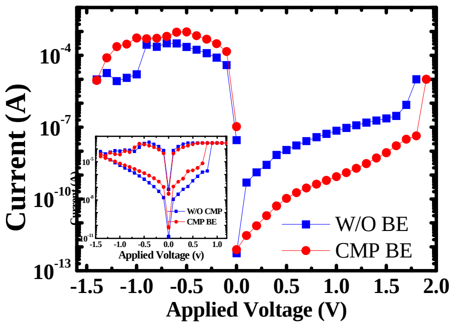

Fig. 7. The typical forming process and first reset *I-V* curves for the devices with or without CBE, the inserted one is the typical BRS characteristics of the devices.

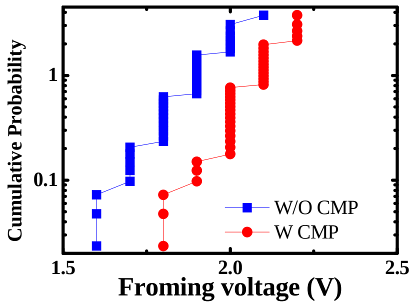

Fig. 8. The Weibull plot of V_F of Ti/HfOx RMs above TiN BE with or without CMP.

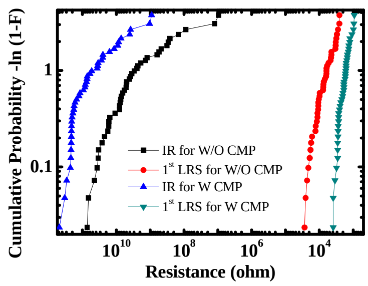

Fig. 9. The Weibull plot of the resistance of IRS and first reset for the devices consisted of HfOx above TiN w/wo CMP.

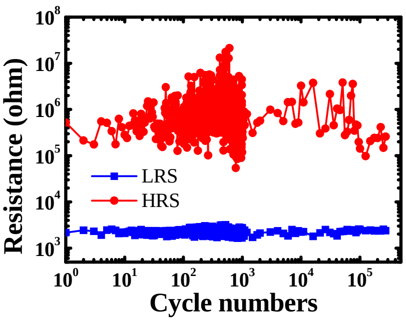

Fig. 10. Endurance of HfOx/TiN memory cell with 1R configuration. The resistance of HRS and LRS for the device can be well resolved after 3×10^5 cycles.

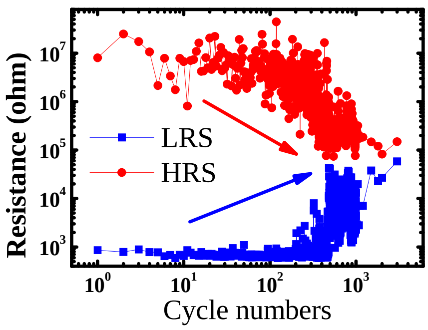

Fig. 11. Endurance of HfOx RM by using TiN CBE with 1R configuration. The resistance of HRS and LRS for the device will be overlapped after 10^3 cycles.

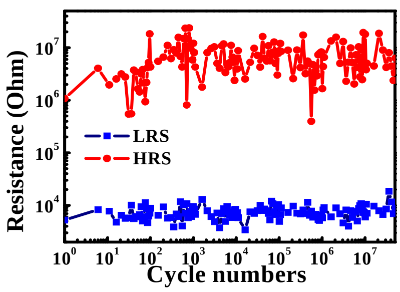

Fig. 12. Endurance characteristics of HfOx resistive memory with 1T1R configuration by using CMP treated TiN BE.

Acknowledgement This work is supported by the National Science Council through Grant No. NSC 99-2221-E-159-023-.